Sethi, Jatin; Farooq, Muhammad; Österberg, Monika; Illikainen, Mirja; Sirviö, Juho Antti

Stereoselectively water resistant hybrid nanopapers prepared by cellulose nanofibers and water-based polyurethane

Published in:
Carbohydrate Polymers

DOI:
10.1016/j.carbpol.2018.07.028

Published: 01/11/2018

Document Version
Peer-reviewed accepted author manuscript, also known as Final accepted manuscript or Post-print

Stereoselectively water resistant hybrid nanopapers prepared by cellulose nanofibers and water-based polyurethane

Jatin Sethi[1], Muhammad Farooq[2], Monika Österberg[2], Mirja Illikainen[1], and Juho Antti Sirviö[1*]

1. Fibre and Particle Engineering, University of Oulu, Oulu, Finland.
2. Department of Bioproducts and Biosystems, Aalto University, Helsinki, Finland.

***Corresponding Author:** Juho Antti Sirviö, **Email:** juho.sirvio@oulu.fi

Abstract

Cellulose nanopapers, known for excellent mechanical properties, loses 90% of their stiffness in the wet conditions. In this study, we attempt to improve the wet mechanical properties of cellulose nanopaper by incorporating polyurethane by a novel and ecofriendly method. Water based PU was dispersed along with CNFs in water and hybrid nanopapers were prepared by draining water under vacuum followed by forced drying. These hybrid nanopapers have a gradient interpenetrating structure with PU concentrated towards one side and CNFs towards the other, which was confirmed by scanning electron microscopy, x-ray photoelectron spectroscopy and contact angle measurements. Because of this, the nanopapers are water resistant on one surface (PU rich side) and hydrophilic on the other (cellulose rich side), making them stereoselectively water resistant. When wetted with water on the PU side, the hybrid nanopaper with 10% PU is able to retain 65% modulus; on the other hand, the reference retains only 10% of the modulus. Similar results are seen in the tensile and the yield strength. Additionally, the hybrid nanopapers have higher elongation than the reference indicating their relevance to the reported material in applications such as flexible

electronics. Finally, the hybrid nanopapers have an improved thermal stability according to TGA results. The reported material is relevant to the applications such as flexible electronics and transparent displays.

Graphical Abstract

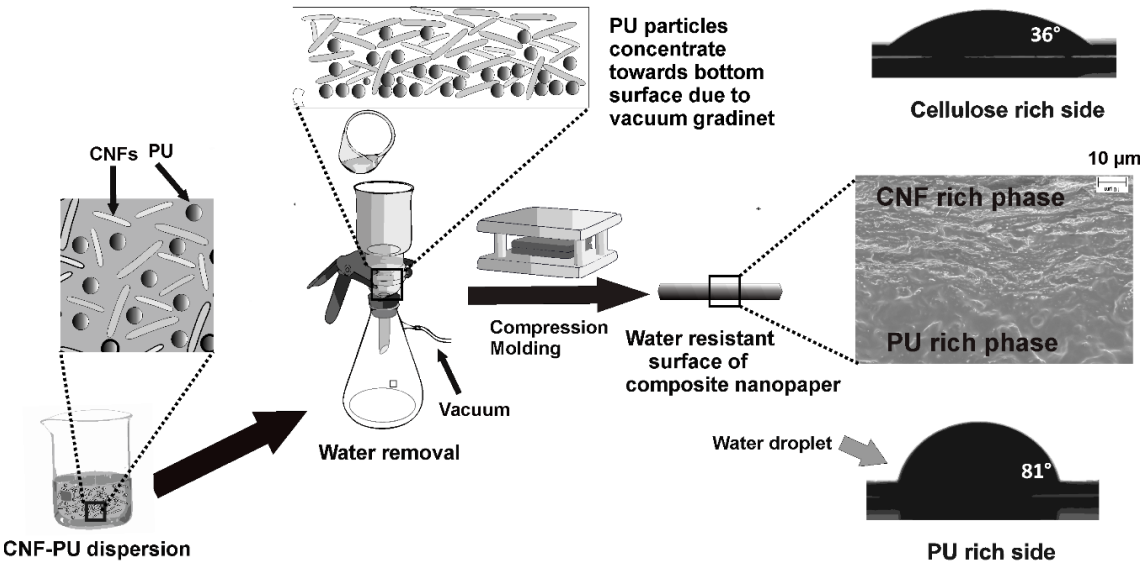

Stereoselectively water resistant composite nanopaper

Keywords: Cellulose nanopapers; Polyurethane; Flexible composites; Hybrid materials; Gradient interpenetrating network; Water resistance.

1 Introduction

Non-degradable plastic materials have dominated the world of materials for almost a century, which until recently, was proudly addressed as the age of plastics. Plastics evolved as a corrosion free, lightweight, durable material for non-structural applications (Greene & Tonjes, 2014). Characteristics with such a stark contrast to corroding and expensive metals skyrocketed their popularity, making them mandatory for everyday materials. In course of modernization and progress, they became irreplaceable. As the population grew, so did the demand and supply of the plastics. The perils of plastics

were ignored for a long time. However, during last couple of decades, it has been realized that such materials are damaging our environment on a massive scale. Plastics are one of the major pollutants produced by us. Plastic has created (and is still creating) a massive amount of landfill deposits. If not lying dormant under the ground, plastics will be floating in the oceans for a long time (Barnes, Galgani, Thompson, & Barlaz, 2009). There is no easy way to get rid of such ultra-stable materials. The hailed durability of plastics is, in fact, a curse in terms of sustainability and environmental protection. Additionally, the crude oil resources are depleting faster than ever (Gamadi, Elldakli, & Sheng, 2014). It has become a matter of paramount interest among the material scientists to find environment- friendly alternatives for the everlasting plastics. A common trend is to combine the synthetic plastic with renewable polymer to obtain a new environment-friendly polymeric material (Kim & Park, 1999; H. J. Lee, Lee, Lim, & Song, 2015).

In search of renewable materials, researchers have refocused on the cellulose, which is the most abundant polymer in the world. Cellulose, a biodegradable polymer, was a major source material for a long time much before industrial revolution (in the form of paper and wood). In search of alternative, new eco-friendly materials, it received a head start as its chemistry is well-documented and understood. Additionally, it was found that nanoscale, cellulose offers exciting opportunities for functional materials (Klemm et al., 2011; Shun Li, Qi, & Huang, 2017) Cellulose, present in form of well-arranged crystallites in amorphous matrix of hemi-celluloses and lignin, is the vital structural element of wood. It has been estimated that elastic modulus of cellulose crystal can be as high as 100-160 GPa (Eichhorn et al., 2010; Mittal et al., 2018). Such fascinating properties of a natural material have persuaded researchers to use this ancient material

in their modern research. Nanocellulose has started an exciting field of research with promising future, but it is certainly not devoid of challenges.

As any new field of research, nanocellulose has brought its own roadblocks, which need to be crossed. The major one was large-scale production in a cost effective way– as grinding pulp to nanosized fibers was a slow and energy consuming process. The problem was solved by using energy-efficient production which involved use of physical, chemical or enzymatic pretreatment of cellulose pulp, followed by homogenization (grinding) (Isogai, 2018; Klemm et al., 2011). Once the feasible production methods were established, the attention was focused on the various aspects of material and its potential uses. One such product is self-standing 100% cellulose film called nanopapers, which are prepared by draining water from cellulose nanofibers (CNFs). They are fascinating as they are known to have an elastic modulus of 10-20 GPa and a strength of 200 MPa (Henriksson, Berglund, Isaksson, Lindström, & Nishino, 2008; Sehaqui et al., 2012), which is unheard of in case of a polymeric material. It has been suggested that in the future, nanopaper will find use in high-end applications such as packaging (Sehaqui, Zimmermann, & Tingaut, 2014), electronic displays (Sehaqui et al., 2014), flexible electronics (Koga et al., 2014), lithium ion batteries (Chun, Lee, Doh, Lee, & Kim, 2011), and transformers (Huang, Zhou, Zhang, & Zhou, 2018) .

Despite such excellent properties and huge potential, nanopapers are still far away from commercialization. One of the major reasons being their poor performance under water (Benítez, Torres-Rendon, Poutanen, & Walther, 2013). When wetted with water, the nanopaper drastically loses its mechanical properties. It has been reported that the modulus of a soaked nanopaper reduces to 95% of the dry value (Sehaqui et al., 2014). Even in the presence of high humidity, the mechanical properties are heavily mitigated

(Benítez et al., 2013). The reason behind this is that the cellulose molecule has pendant hydroxyl groups that make the surface hydrophilic. As a result, water seeps into the interfibrillar region of the nanopaper and causes the nanofibers to slide easily under external load leading to poor mechanical properties (Benítez et al., 2013). We found that this issue, understandably an important one, has rarely been discussed in literature. Sehaqui et al. modified nanofibers by grafting them with alkyl chains through esterification (Sehaqui et al., 2014). The presence of hydrophobic chains instead of hydrophilic hydroxyl group rendered the resulting nanopaper hydrophobic with 20-fold improvement in wet strength as compared to a reference. Recently, we used lactic acid modification to improve the water resistance and dimensional stability of nanopapers (Sethi, Farooq, et al., 2018). In this research, we hypothesized that using nanoscale polymer particles in tandem with cellulose nanofibers would be a possible way of preparing nanopapers with improved water resistance. It was decided to use water-based latexes as they are already stable in an aqueous suspension and have a nanoscale particle size (Product center coatings Covestro, 2018). The idea was to combine a renewable material (cellulose) with a synthetic polymer to prepare a superior hybrid material with minimal environmental impact. The structure was inspired by wood, which is more than 50% cellulose and still water resistant, due to the presence of lignin that gives it its extraordinary strength even in rain. Biomimicking is an interesting approach to prepare advanced materials. Nature has found a perfect way to make natural materials to particular standards. The key to commercialization of such materials can be in seeking inspiration from nature.

This paper presents a water-based method to prepare polyurethane (PU) –CNF hybrid nanopapers from a water based method. A commercially available PU dispersion (Bayhydrol® UH 240) and a CNF suspension was combined and water was drained to

make nanopapers with PU concentration of around 1 wt.-%, 10 wt.-%, 30wt.-% and 60wt.-%. The morphology was analyzed by scanning electron microscopy. X-ray photoelectron spectroscopy (XPS) and contact angle measurements were used to characterize the surface properties. Tensile testing (dry and wet) was used to evaluate the mechanical properties and Thermogravimetric analysis (TGA) was used to evaluate the thermal stability. The papers prepared were significantly more water-resistant than the reference and were also thermally stable. The hybrid nanopaper containing relatively small amount (10 wt.-%) of non-biodegradable polymer exhibited superior properties compared to reference nanopaper from pure CNF.

2 Materials and methods

Bayhydrol® UH 240 (henceforth, referred to as UH 240), an anionic surfactant based polyurethane dispersion was kindly provided by Covestro. The characteristics of UH 240 are provided in Table S1 (supplementary file). Cellulose nanofibers were prepared from softwood sulfite pulp provided by Stora Enso (Oulu, Finland). For grinding, pulp with a concentration of 1.6 wt.-% was fed to a Masuko grinder. The initial contact mode was 0-point, and the distance was gradually decreased from - 20 (3 passes), - 40 (4 passes), - 60 (5 passes) and - 90 (7 passes). The chemical composition of the reference pulp was 95.0 wt.-% cellulose, 4.2 wt.-% hemicellulose, 0.3 wt.-% lignin and 0.5 wt.-%. L-(+)-Lactic acid (80%) was purchased from Sigma-Aldrich.

2.1 Preparation of nanopaper

CNF suspension was diluted to a concentration of 0.2 wt.-% and UH240 was added to obtain a proportion of CNF to PU as 95:5, 80:20, 50:50 and 30:70. The CNF-PU suspension was mixed with a high speed ultraturrax at 10000 rpm. Lactic acid (equal to amount of dry CNF) was used as additive to reduce the draining time. The sample was

139 sonicated till the energy imparted was 300 J/ml. The details of this method is reported
140 elsewhere (Sethi, Oksman, Illikainen, & Sirviö, 2018).

141 The nanopapers were prepared by filtering the suspension of CNFs and UH 240 through
142 a Durapore PVDF membrane filter (Fisher Scientific, Pittsburgh, USA) with a pore size
143 0.65 µm. The vacuum was kept at 70 ±5 kPa. Before filtration, the suspension was
144 degassed under a vacuum of 70 kPa for half an hour. The wet CNF-PU sheet was peeled
145 off from the PVDF membrane and kept between two steel mesh cloths (mesh size 70
146 µm), along with absorbent papers and carrier boards. The whole assembly was kept in
147 compression molding at a temperature of 100 °C and a pressure of 5 MPa for 30
148 minutes. For composites with PU concentration higher than 50 wt.-%, PU was in a
149 major phase and was infused into the steel mesh under higher temperature and pressure.
150 Therefore, the pressure was reduced to 0.5 MPa to aid the film formation, once the film
151 was dry, the steel mesh was removed and the films were compressed at 5 MPa for 30
152 minutes. The coding of the samples was done according to the amount of PU in the final
153 film. It was observed that some PU was filtering through the PVDF membrane, perhaps
154 due to its spherical morphology and the high vacuum. Therefore, the PU fraction was
155 determined by calculating the increase in weight in comparison to the reference CNF
156 film. The final samples were named as CNF(1)PU, CNF(10)PU, CNF(30)PU and
157 CNF(60)PU, where the number in brackets refer to the actual concentration of PU in the
158 film.

159 **2.2 Characterization**

160 2.2.1 Scanning electron microscopy

161 Zeiss Ultra Plus (Oberkochen, Germany) field emission scanning electron microscope
162 (FE-SEM) was used for studying the morphology of hybrid nanopapers. The in-lens

detector was used to collect signals from platinum coated samples after scanning the sample with an electron beam and an acceleration voltage of 5 kV.

2.2.2 X-ray photoelectron spectroscopy

Thermo Fisher Scientific ESCALAB 250Xi X-ray photoelectron spectroscopy (XPS) system was used for conducting chemical surface analysis. XPS spectra were collected using monochromatic Al Kα (1486.6 eV) beam. Survey scan pass energy of 150 eV using 1 eV step and High-resolution scan pass energy of 20 eV was with 0.1 eV was used along with charge compensation by ion bombardment. The analysis chamber pressure was about 3×10^{-9} mbar.

2.2.3 Water contact angle

CAM 200 (KSV Instruments Ltd, Finland) was used for contact angle measurements. A 6.5 µL drop of Milli-Q water was placed on both sides of the surface, and 60 images were captured via the CCD camera (1 image/sec). The contact angle was determined by the software provided by the instrument manufacturer. Three measurements at different positions were made and the average values with standard deviation are reported.

2.2.4 Mechanical properties

Tensile testing of the samples was done using Instron 5544 universal material testing machine (Norwood USA). Strips (50mm x 5 mm) were cut from the hybrid and reference nanopapers and stored in controlled environment chamber for at least 96 hours before testing, which was maintained at a humidity of 50% and a temperature of 23 °C. The tests were conducted using a 100 N load cell, and the crosshead speed was 2 mm/minute. The distance (gauge length) between the grips was 3 mm. The elastic modulus was calculated from the slope of the stress-strain curve in the linear region of the curve with the help of Origin software. The results are reported as an average of minimum of 5 samples. The same tensile testing parameters and equipment was used

for wet tensile testing, which was planned on the basis of procedure described by Sehaqui et al. (Sehaqui et al., 2014). Briefly, a drop of 50 µl was carefully placed on the middle of the strips (50 mm x 5 mm). Stress-strain curves were recorded after 60 seconds of wetting and the results are reported as an average of three samples. The procedure was recorded on both sides to test the water resistance of both the surfaces. Wet by dry stiffness ratio (E_{wet}/E_{dry}) was used to compare the modulus reduction in different samples.

2.2.5 Swelling studies

Swelling studies were conducted to measure the water absorption. Samples were dipped in the water overnight and the increase in weight was recorded. Before weighing, the excess water was removed by pressing samples in blotting paper.

2.2.6 Thermal stability

Thermogravimetric analysis (TGA) of the hybrid nanopapers was conducted with the aid of TA-TGA Q500 (New Castle, USA). 10 mg sample was heated in platinum pan till a temperature of 900 °C was reached under the nitrogen atmosphere, with a heating rate of 10 °C /min.

3 Results and discussion

3.1 Morphology

Introduction of PU in the nanopaper led to significant change in the morphology as observed in Figure 1 (a,b, and c), which shows FESEM images of the cross-section of samples fractured in tensile testing. Both the reference and the hybrid nanopapers have a layered structure, which is characteristic of cellulose nanopapers. However, in the hybrid nanopapers, the contrast due to the presence of PU is obvious, especially, in CNF (30) PU where the CNF layers are seen well-embedded in the PU matrix. Additionally,

212 there is a difference in the phase structure of PU and CNFs across the cross-section.
213 There is a PU rich phase towards the top surface and a CNF rich phase towards the
214 bottom surface (CNF(30)PU). The preferential presence of PU towards one surface is
215 confirmed by FESEM images of the surface (Figure 1(d, e, and f), which presents the
216 surface morphology of the CNF(10)PU hybrid nanopaper (both surface; Figure 1e and
217 f) and reference nanopaper (Figure 1d). Interestingly, CNF fibers are visible on one of
218 the surfaces on hybrid nanopaper, which is much the same as it is in reference
219 nanopaper. However, on the other surface of CNF(10)PU, the characteristic fibrous
220 surfaces of CNF are not observed. The images also indicate that the PU is uniformly
221 distributed among the fibers, and doesn't form a mere coating.

222 The shape of the PU and the CNF particles in suspension might explain the preferential
223 migration of PU towards one of the surfaces. PU is present as spherical particles while
224 CNFs are fibrous entities. When mixed together to form a suspension in water, they will
225 be equally distributed. However, when the water is drained through the PVDF
226 membrane to make nanopaper, CNFs are retained on the membrane to form a fibrous
227 network structure caused by "concentration induced aggregation and floc
228 formation"(Benítez et al., 2013). On the other hand, PU particles are in spherical shape
229 and under the influence of vacuum gradient, they are likely to get sucked through the
230 CNF web as particles though a membrane, thus concentrating towards the membrane
231 and resulting in a PU rich phase. The whole system can be seen as an intricate network
232 of CNFs embedded in a matrix of PU, which forms its own network, with concentration
233 varying along the cross-section. This kind of formation is called a gradient based
234 interpenetrating network, where concentration of individual components varies across
235 the cross-section (Lipatov & Karabanova, 1995).

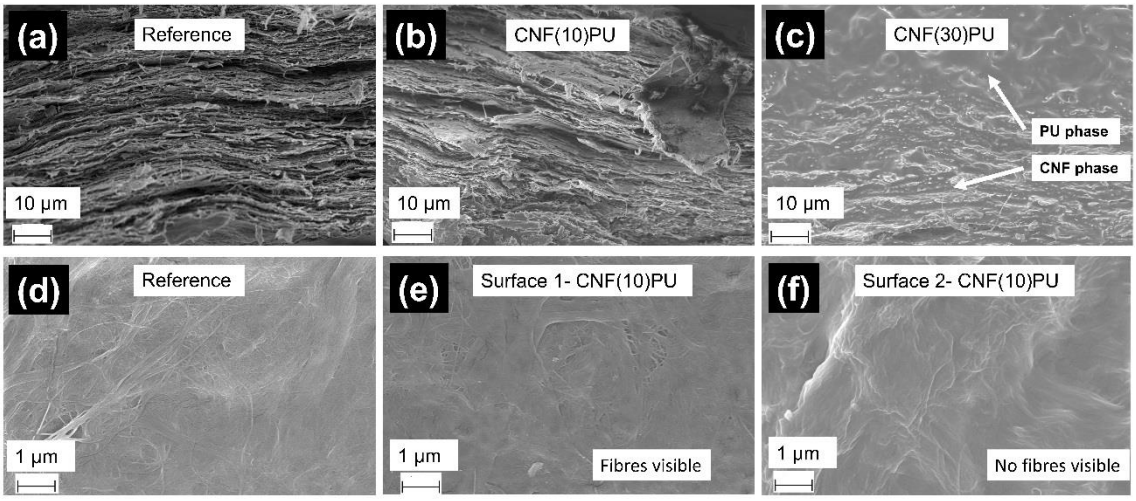

Figure 1 (a), (b), and (c). The layered structure of the reference and hybrid nanopapers (CNF(10)PU and CNF(30)PU. Impregnation of the CNF structure by PU is clearly visible in CNF(30)PU. (d), (e), and (f) FESEM images of surface of reference nanopaper and both, CNF rich and PU rich, surfaces of CNF(10)PU. The reference and the surface 1 (CNF rich) of CNF(10)PU have the same surface profile where fibres are visible, while in the surface 2(PU rich) of CNF(10)PU, there are no fibers visible indicating that PU is accumulated towards that surface.

3.2 X-ray photoelectron spectroscopy

The XPS analysis confirms that PU is preferably concentrated towards one surface. XPS was used for surface analysis in this study because it is a surface specific method, which characterizes the 0–10 nm of top section of material (H.-L. Lee & Flynn, 2006). The relative concentration of nitrogen atoms on the surface of the pure CNF, neat PU and hybrid nanopapers (CNF(10)PU and CNF(30)PU) are shown in Figure 2. It confirms that nitrogen atoms are present at a higher concentration towards one surface than on the other. The complete quantitative results of XPS analysis are presented in Table S2(supplementary file). The PU rich surface of CNF(10)PU has a nitrogen concentration of 1.19 %, and for the CNF rich side, the concentration is 0.4 %. A similar pattern of distribution can be seen in the CNF(30)PU. XPS could be used to determine the presence of PU for it has a peculiar chemical structure as compared to the other polymers. PU has nitrogen atom in the polymer chain; on the other hand, cellulose has none. The chemical structures of PU and cellulose and Lactic acid (additive) are

258 presented in Figure S2 (supplementary file). XPS results confirm the differential

259 distribution of PU across the cross-section as indicated by the SEM pictures (Figure 1).

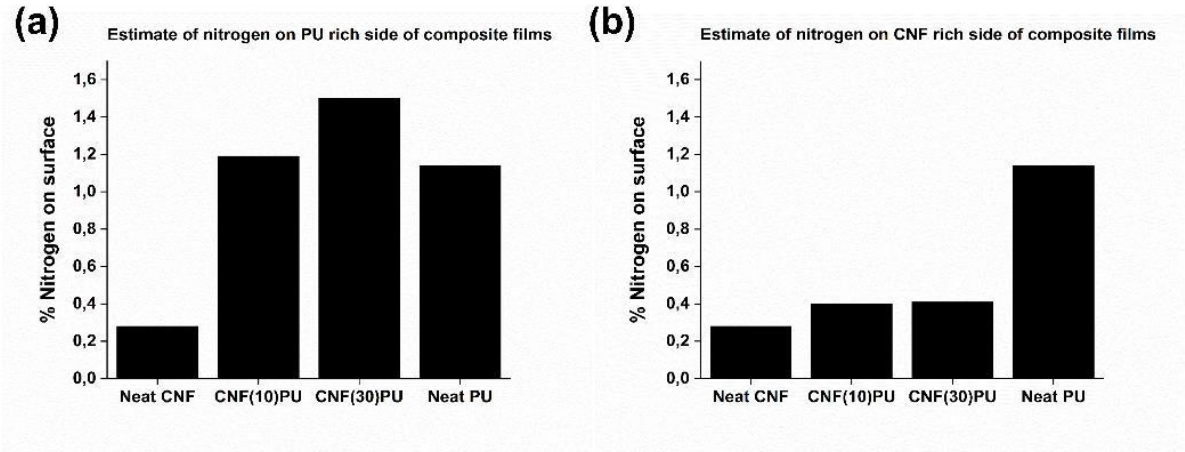

260

261 Figure 2 Distribution of nitrogen atoms in neat CNF, neat PU, CNF(10)PU (both sides),
262 and CNF(30)PU (both sides).

263 The detailed XPS spectra of neat CNF, neat PU, CNF(10)PU (PU and cellulose side) is

264 provided in the Figure 3. The peak PU representing the chemical group –N-C=O is

265 known to appear at 289 eV (Yang et al., 2001), which can be clearly seen in the PU side

266 of CNF(10)PU (marked by red color). On the other hand, the intensity of same peak is

267 significantly less on cellulose side, indicating that PU is present but in less quantity.

268 Similar results were observed for (C-O) peak of CNF which is usually observed at 286

269 eV (Liao et al., 2016), indicating the presence of CNF on both sides; more towards CNF

270 side and less towards PU side. Another prominent observation from that figure is that

271 that NCO bonds are more dominating in PU side and CO bonds on CNF side; yet both

272 have elements corresponding to presence of both CNF and PU.

273 It is worth mentioning that the neat CNF (reference) sample also gave a nitrogen signal

274 in XPS, though the concentration was merely 0.28%. The peak from nitrogen in

275 reference was at 399.8 eV while in PU was 399.2 eV, indicating that the bonding

structure of nitrogen in CNF is different in the samples. Therefore, it is not the result of PU contamination. Perhaps, some additive or impurity was present in the supplied pulp.

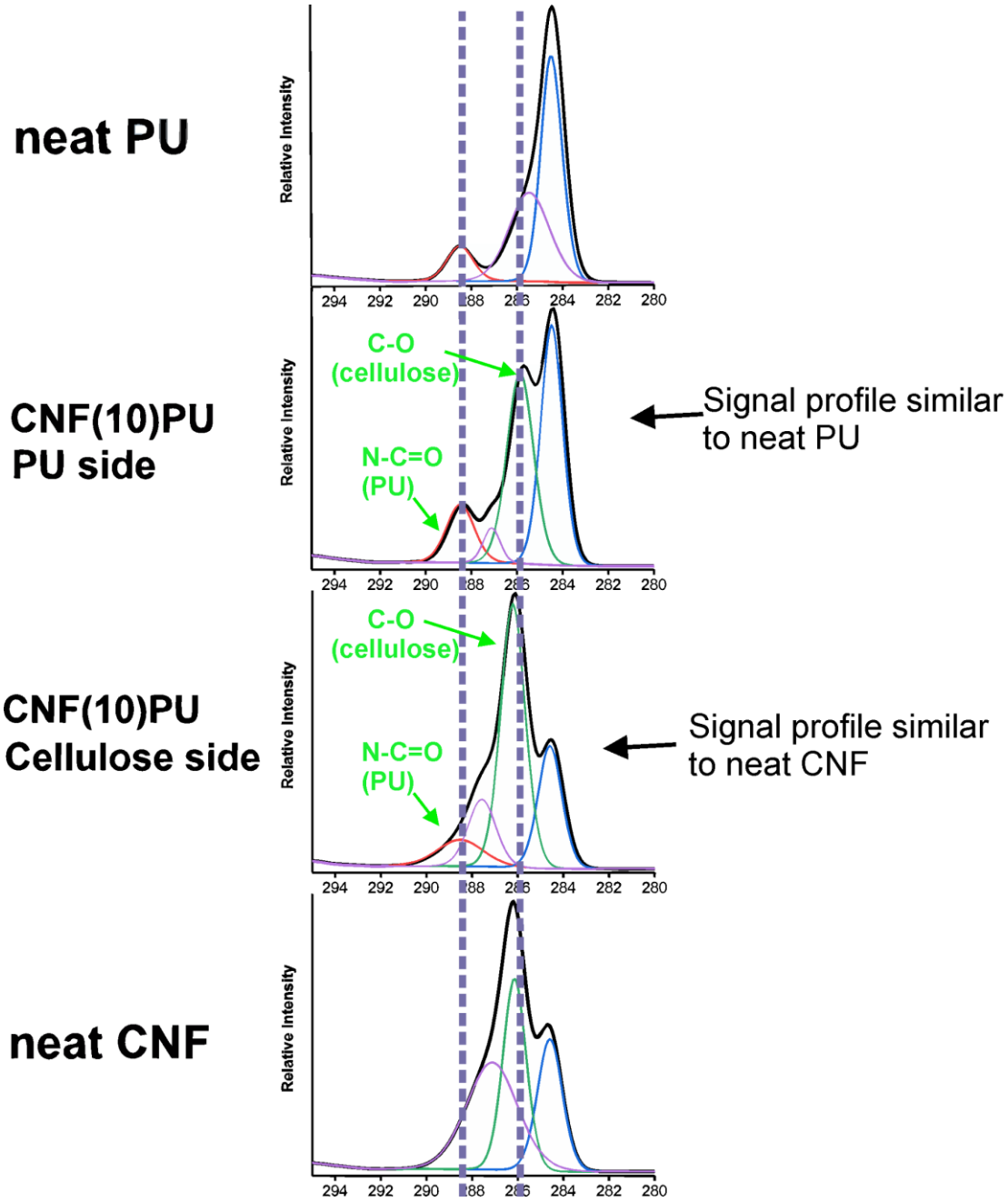

Figure 3 Detailed XPS spectra of neat PU, CNF(10)PU (PU side and cellulose side), and neat CNF. Clearly, the PU side of hybrid nanopaper have more concentration of PU than cellulose side. Additionally, the PU side is similar to neat PU and cellulose side is similar to neat CNF.

3.3 Contact angle

The PU rich surface of hybrid nanopapers had significantly different contact angle than the other surface (Figure 4). For the CNF(10)PU nanopaper, the contact angle with water is 81° on PU rich side; however, on the CNF rich side it is merely 36 °, indicating the water resistance of the PU rich surface. CNF(30)PU sample, showed a similar pattern with a difference of almost 25 degrees in contact angle on both sides (63° on PU rich side and 36° on CNF rich side). The contact angle of neat CNF was 46° and of neat PU was 81°. The values of contact angles (with standard deviation) of hybrid nanopapers along with neat CNF and neat PU is provided in Table S3 (supplementary file).

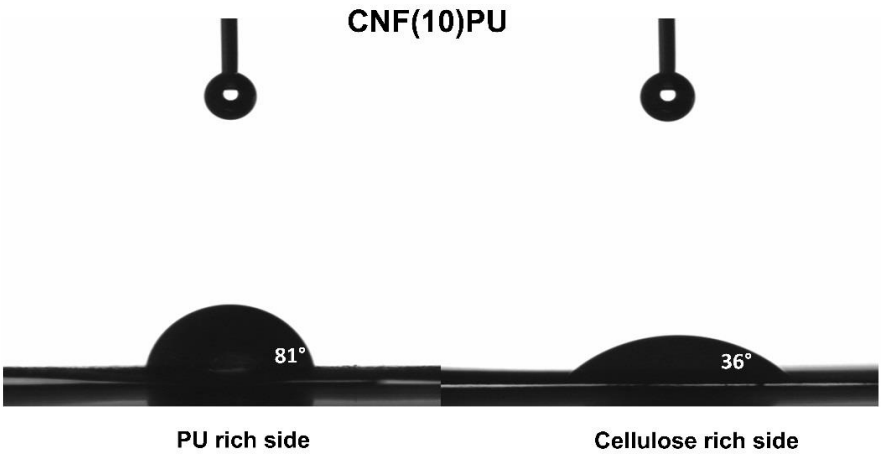

Figure 4 Photographic images of the contact angle measurements. The PU rich side has a considerably higher angle than the CNF rich side.

It is worth mentioning that achieving a high contact angle on cellulose nanopaper is a demanding task. (Sehaqui et al., 2014) grafted different length carbon moieties through esterification in acetone medium. They achieved a contact angle of 79° when the chain length was 6 carbons long. For 4 carbon moiety, it was 57° and for 2 carbon, it was 32°. Only 16 carbon molecule gave the angle of 118°. Additionally, (Peresin et al., 2017) aminated and silylated the CNF film to achieve a contact angle of 60° and 70°. We were

able to achieve a contact angle of 81° without using complicated process and hazardous reagents. This is an added advantage.

3.4 Mechanical Properties

The introduction of PU in the CNF network is causing a decrease in the elastic modulus (E), which is shown in Figure 5 (quantitative results in Table 1). The decrease in the elastic modulus of hybrid nanopapers with a PU content of 1 wt.-%, 10wt.-%, 30 wt.-% and 60 wt.-% was 9%, 20 %, 50%, and 70% respectively in comparison to reference. This can be explained by the properties of the neat PU, which is highly elastomeric in nature (more than 700% elongation) and has a modulus of 0.003 GPa, which is vastly lower than that of the reference nanopaper. Introducing such an elastomeric polymer in a stiff CNF network is likely to result in the loss of modulus.

Another aspect of the hybrid nanopapers that can be observed in Figure 5 is the higher elongation when comparing to the reference nanopaper. It increased approximately by 1% in the CNF(1) PU and the CNF(10) PU samples. It can again be explained by the high elongation of neat PU. This is quite interesting. Usually, introduction of a polymer in a nanopaper leads to reduction in elongation, Although it leads to a higher modulus (Sethi, Farooq, et al., 2018) (Henriksson & Berglund, 2007), the high elongation in the reference nanopaper is due to the sliding of nanofibrils. If a polymer is introduced, it strengthens the structure by embedding the fibers in a matrix and reducing the porosity. However, introduced polymer leads to decrease in the elongation polymers, thus restricting sliding of CNFs, which is a known reason for the inelastic extension of the nanopaper (Henriksson et al., 2008). In our results, the polyurethane, being highly elastomeric in nature, is acting in tandem with the CNFs, as result the elongation is not lost. It can be speculated that when the fibrils slide, the PU matrix keeps the CNF

network together even at high elongation. This is an added advantage of the reported material as flexibility is required in applications such as flexible electronics (Shaohui Li & Lee, 2017). The results are promising as the nanopapers have combination of properties from both the constituent materials. The cellulose rich side can be used for the growth of conductive films and polymer rich surface could protect the conductive nanopaper against water as shown in the next section.

Table 1 Quantitative results of stress-strain analysis of the reference and hybrid nanopapers.

	modulus (Gpa)	tensile strength	Elongation
Reference	7.8 ± 0.6	155 ± 12	6.9 ± 1.3
CNF(1)PU	7.1 ± 0.1	143 ± 11	8.2 ± 1.2
CNF(10)PU	6.2 ± 0.4	126 ± 9	7.9 ± 0.7
CNF(30)PU	4.1 ± 0.2	46 ± 7	2.5 ± 1.1
CNF(60)PU	2.3 ± 0.2	44 ± 1	6.3 ± 0.5
Neat PU	0.003	1.4 ± 0.3	> 700%

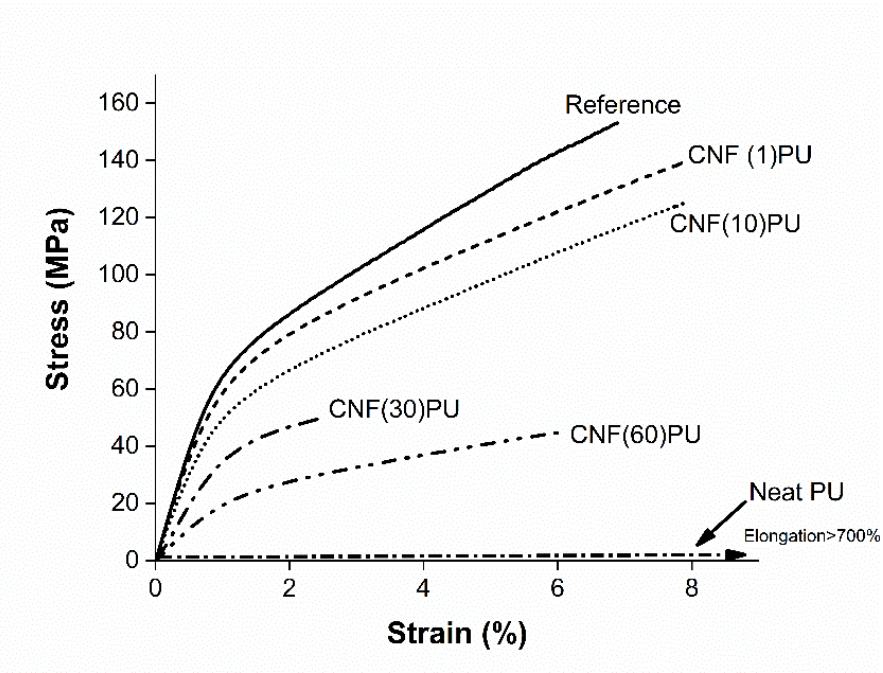

Figure 5. The stress-strain curves of the hybrid and reference nanopapers. PU is extremely elastomeric, due to which the hybrid nanopaper are losing their moduli.

Water based polyurethane dispersions are quite versatile and find use in commercial applications such as adhesives and coatings. They are prepared by reacting dihydroxy alchohol with diisocyanate to form a prepolymer, which is further reacted with chain extender to increase the molecular weight. This is later transferred to water medium to form a water dispersion(Tennebroek et al., 2018) (Yoon Jang, Kuk Jhon, Woo Cheong, & Hyun Kim, 2002)(Subramani, Cheong, & Kim, 2004)(Chang et al., 2017). The schematic depiction of water based polyurethane is provided in Figure S1 (supplementary file).

3.5 Wet tensile testing

The hybrid nanopapers were water resistant on the PU rich side. Stress-strain curves of wetted samples on the PU side are shown in Figure 6a (quantitative results in Table 2). CNF(10)PU sample outperformed all the other samples in the elastic modulus, elongation, tensile strength and yield strength values, while the reference nanopaper had the poorest mechanical properties in wet conditions. 90 % of its modulus was lost (from 7.8 GPa to a 0.8 GPa) in wet state. On the other hand, the CNF(10)PU sample lost only 35% of its modulus (down from 6.9 GPa to 3.9 after wetting). The modulus of CNF(10)PU was 400% higher than reference nanopaper (in wet state). Other hybrid nanopapers also had superior water resistance as compared to the reference nanopaper. CNF(1)PU, CNF(30)PU, CNF(60)PU had respectively 150%, 300% and 100% higher modulus than the reference, respectively. The E_{dry}/E_{wet} values are presented in Table 2. Similar trend was observed in tensile strength, yield strength and elongation with CNF(10)PU outperforming the other samples.

The CNF side of the hybrid nanopapers did not show any significant improvement in the wet state mechanical properties. Figure 6(b) shows a column graph of the elastic

modulus of the CNF(10)PU samples, which were wet from the CNF rich side along with the reference nanopaper. Elastic modulus of the hybrid nanopaper was marginally improved over wetted reference nanopaper indicating the susceptibility of cellulose when in contact with the water. Same hybrid nanopaper (CNF(10)PU) when wetted on the PU side, was able to maintain the stiffness and ended up at 4 GPa, indicating the advantage offered by PU when it comes to water resistance.

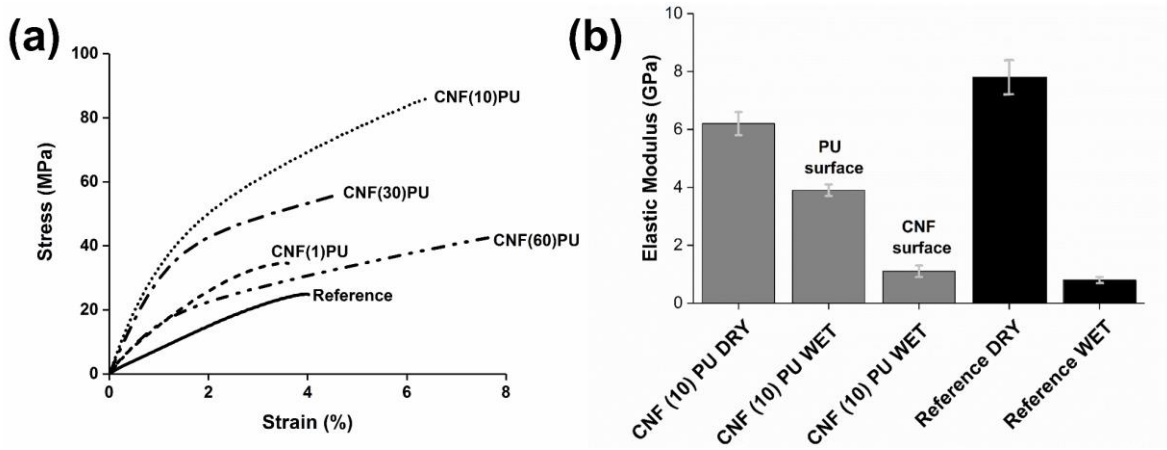

Figure 6 (a). Stress-strain curves of the wetted samples hybrid nanopapers (wetted on the PU rich side). All the hybrid nanoapers have superior mechanical properties superior to the refernce nanopaper., (b). Comparision of the elastic moduli of the wetted CNF(10)PU (both sides) and the refernece. Dry CNF(10)PU and dry reference modulus are also enlisted. The presence of PU is benefical for safeguarding of elastic modulus under the influence of water

Table 2. Evolution of the elastic modulus of reference and hybrid nanopapers before and after wetting. Ewet/Edry and % decrease is also enlisted.

	Elastic Modulus			
	Before wetting	After wetting	E_{wet}/E_{dry}	% decrease
Reference	7.8	0.8	0.1	90
CNF(1)PU	7.1	2	0.3	70
CNF(10)PU	6.2	3.9	0.6	35
CNF(30)PU	4.1	3.3	0.8	20
CNF(60)PU	2.3	1.7	0.75	25

(Sehaqui et al., 2014) used surface grafting of long chain carbon molecules to improve the wet properties. Only the 16 carbon chain moiety showed a noticeable improvement (E_{wet}/E_{dry} = 0.5). Other carbon chains gave E_{wet}/E_{dry} value less than 0.13. The method reported in this study E_{wet}/E_{dry} values as high as 0.8 (and minimum 0.3) without the use of hazardous reagents.

3.6 Swelling studies

The water resistance of the hybrid nanopapers was confirmed by the swelling studies. The results are presented in Figure 7. All the hybrid nanopapers had lower water absorption than the reference indicating that the presence of PU is making hybrid nanopapers water-resistant. CNF(30)PU and CNF(60)PU absorbed the least amount of water: 36% and 33% respectively, which is approximately 60% less than the reference. The difference is more prominent in CNF(30)PU and CNF(60)PU as PU has properly embedded the CNFs (as seen in Figure 1). On the other hand, PU Matrix is not clearly visible in CNF(10)PU. The reason behind the reduced water absorption might be that the presence of PU that is separating a fraction of the CNFs from the environment, which makes them impervious to water. The findings from the swelling studies indicate the basic tendency of the hybrid nanopapers to constrain the water uptake by the CNFs.

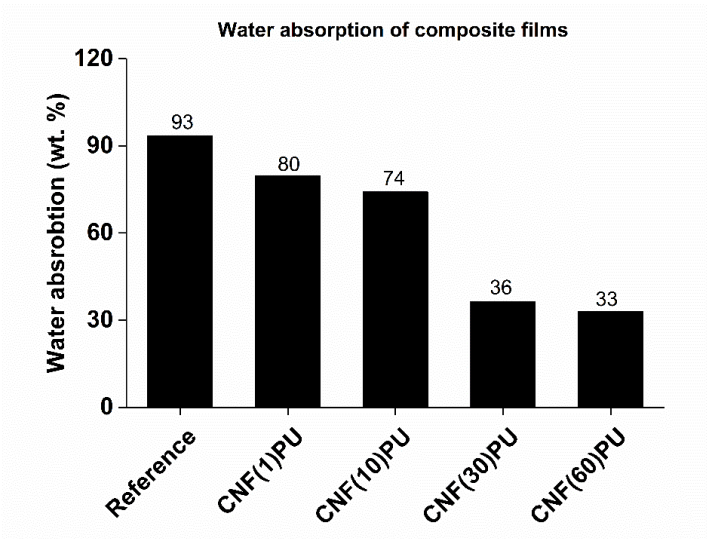

Figure 7. Water absorption of the hybrid and reference nanopapers. All the composites nanopapers have less water absorption than reference.

3.7 Thermal Stability

The CNF(60)PU and CNF(30)PU hybrid nanopapers are more thermally stable than the reference, as seen in Figure 8(a), which presents the thermograms from the thermogravimetric analysis (TGA). The thermal properties of CNF(10)PU are comparable with those of the reference. Quantitatively, the reference is losing 48% of its weight between 0 and 350°C. CNF(60)PU on the other hand, lost only 22% of its weight at the same temperature, indicating its superior thermal properties. CNF(10)PU and CNF(30)PU, respectively lost 42% and 41% of their weight, which is better than the reference. The influence of the presence of PU is more clearly observed in Figure 8(b), which presents the differential weight loss thermograms indicating the percent weight loss per degree Celsius. The CNF has the highest rate of degradation around 350 °C, PU on the other hand has it at 410 °C. As the amount of PU is increasing, the degradation peak of PU is becoming higher, indicating that more material is degrading above 400 °C. It also confirms the presence of two separate phases: one PU rich and the other CNF rich.

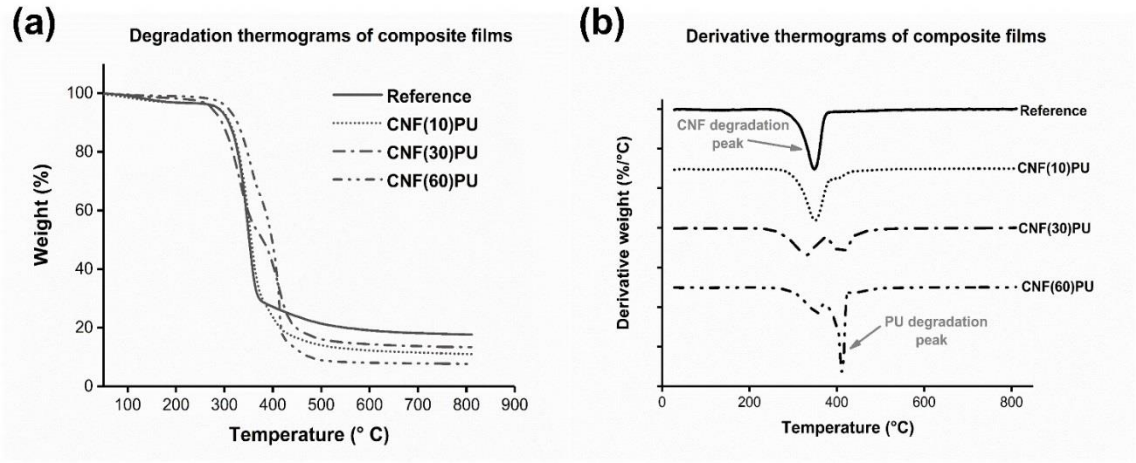

Figure 8 (a). Degradation thermograms of the reference and hybrid nanopapers indicating the thermal stability of hybrid films. (b). Derivative thermograms of reference and hybrid nanopapers indicating the peak degradation temperature of CNF and PU phase. CNF phase degrades around 350°C and PU phase around 410°C.

4 Conclusion

This research provides an eco-friendly water based approach to prepare hybrid nanopapers from PU and CNFs. Nanopapers with PU content as high as 60% were prepared from commercially available PU latex. Interestingly, the PU particles were migrating, through the CNF web, towards the applied vacuum due to a spherical morphology and a small particle size (200 nm). This resulted in formation of gradient interpenetrating network due to preferential accumulation of PU towards one of the surfaces, resulting in separate PU rich and CNF rich phases. The PU rich surface was water resistant with the CNF(10)PU sample retaining its mechanical properties under wet conditions. The modulus of wetted CNF(10)PU was 400% of that of the wetted reference, though originally the reference had a higher modulus. It was found that CNF(10)PU has the most optimal properties achieved with the lowest possible concentration of non-degradable PU. The introduction of PU also led to an increase of thermal stability. Further work studying the use of different polymers such as PMMA and the effect of polymer particle size is at a planning stage.

5 Acknowledgements

The authors acknowledge the contribution of Tommi Kokkonen and Santtu Heinilehto for their contribution in TGA and XPS respectively. This research did not receive any specific grant from funding agencies in the public, commercial or non-profit sectors.

6 References

Barnes, D. K. a, Galgani, F., Thompson, R. C., & Barlaz, M. (2009). Accumulation and fragmentation of plastic debris in global environments. *Philosophical Transactions*

of the Royal Society of London. Series B, Biological Sciences, *364*(1526), 1985–1998. http://doi.org/10.1098/rstb.2008.0205

Benítez, A. J., Torres-Rendon, J., Poutanen, M., & Walther, A. (2013). Humidity and multiscale structure govern mechanical properties and deformation modes in films of native cellulose nanofibrils. *Biomacromolecules*, *14*(12), 4497–4506. http://doi.org/10.1021/bm401451m

Chang, M. T., Lee, J. Y., Rwei, S. P., Wu, W. Y., Chiang, W. Y., Chang, S. M., & Pan, Y. H. (2017). Effects of NCO/OH ratios and polyols during polymerization of water-based polyurethanes on polyurethane modified polylactide fabrics. *Fibers and Polymers*, *18*(2), 203–211. http://doi.org/10.1007/s12221-017-6382-x

Chun, S. J., Lee, S. Y., Doh, G. H., Lee, S., & Kim, J. H. (2011). Preparation of ultrastrength nanopapers using cellulose nanofibrils. *Journal of Industrial and Engineering Chemistry*, *17*(3), 521–526. http://doi.org/10.1016/j.jiec.2010.10.022

Eichhorn, S. J., Dufresne, a., Aranguren, M., Marcovich, N. E., Capadona, J. R., Rowan, S. J., … Peijs, T. (2010). *Review: Current international research into cellulose nanofibres and nanocomposites*. *Journal of Materials Science* (Vol. 45). http://doi.org/10.1007/s10853-009-3874-0

Gamadi, T. D., Elldakli, F., & Sheng, J. J. (2014). Compositional simulation evaluation of EOR potential in shale oil reservoirs by cyclic natural gas injection. In *Unconventional Resources Technology Conference*. Unconventional Resources Technology Conference.

Greene, K. L., & Tonjes, D. J. (2014). Degradable plastics and their potential for affecting solid waste systems. *WIT Transactions on Ecology and the Environment*, *180*, 91–102. http://doi.org/10.2495/WM140081

Henriksson, M., & Berglund, L. A. (2007). Structure and properties of cellulose nanocomposite films containing melamine formaldehyde. *Journal of Applied Polymer Science*, *106*(4), 2817–2824. http://doi.org/10.1002/app.26946

Henriksson, M., Berglund, L. A., Isaksson, P., Lindström, T., & Nishino, T. (2008). Cellulose nanopaper structures of high toughness. *Biomacromolecules*, *9*(6), 1579–1585. http://doi.org/10.1021/bm800038n

Huang, J., Zhou, Y., Zhang, L., & Zhou, Z. (2018). Study on the electrical properties of nanopaper made from nanofibrillated cellulose for application in power equipment. *Cellulose*, *25*(6), 3449–3458. http://doi.org/10.1007/s10570-018-1782-7

Isogai, A. (2018). Development of completely dispersed cellulose nanofibers. *Proceedings of the Japan Academy, Series B*, *94*(4), 161–179.

Kim, Y. J., & Park, O. O. (1999). Miscibilities and biodegradability properties of poly(butylene succinate)-poly(butylene terephthalate) blends. *Journal of Environmental Polymer Degradation*, *7*(1). http://doi.org/10.1002/(SICI)1097-4628(19990516)72:7<945::AID-APP10>3.0.CO;2-0

Klemm, D., Kramer, F., Moritz, S., Lindström, T., Ankerfors, M., Gray, D., & Dorris, A. (2011). Nanocelluloses: A new family of nature-based materials. *Angewandte Chemie - International Edition*, *50*(24), 5438–5466. http://doi.org/10.1002/anie.201001273

Koga, H., Nogi, M., Komoda, N., Nge, T. T., Sugahara, T., & Suganuma, K. (2014). Uniformly connected conductive networks on cellulose nanofiber paper for transparent paper electronics. *NPG Asia Materials*, *6*(3), e93. http://doi.org/10.1038/am.2014.9

Lee, H.-L., & Flynn, N. T. (2006). X-ray photoelectron spectroscopy. In *Handbook of*

Applied Solid State Spectroscopy (pp. 485–507). Springer.

Lee, H. J., Lee, H. K., Lim, E., & Song, Y. S. (2015). Synergistic effect of lignin/polypropylene as a compatibilizer in multiphase eco-composites. *Composites Science and Technology*, *118*, 193–197. http://doi.org/10.1016/j.compscitech.2015.08.018

Li, S., & Lee, P. S. (2017). Development and applications of transparent conductive nanocellulose paper. *Science and Technology of Advanced Materials*, *18*(1), 620–633. http://doi.org/10.1080/14686996.2017.1364976

Li, S., Qi, D., & Huang, J. (2017). Natural cellulose based self-assembly towards designed functionalities. *Current Opinion in Colloid & Interface Science*.

Liao, Q., Su, X., Zhu, W., Hua, W., Qian, Z., Liu, L., & Yao, J. (2016). Flexible and durable cellulose aerogels for highly effective oil/water separation. *RSC Adv.*, *6*(68), 63773–63781. http://doi.org/10.1039/C6RA12356B

Lipatov, Y. S., & Karabanova, L. V. (1995). Gradient interpenetrating polymer networks. *Journal of Materials Science*, *30*(10), 2475–2484.

Mittal, N., Ansari, F., V, K. G., Brouzet, C., Chen, P., Larsson, P. T., … Kotov, N. A. (2018). Multiscale Control of Nanocellulose Assembly : *ACS Nano*. http://doi.org/10.1021/acsnano.8b01084

Peresin, M. S., Kammiovirta, K., Heikkinen, H., Johansson, L. S., Vartiainen, J., Setälä, H., … Tammelin, T. (2017). Understanding the mechanisms of oxygen diffusion through surface functionalized nanocellulose films. *Carbohydrate Polymers*, *174*, 309–317. http://doi.org/10.1016/j.carbpol.2017.06.066

Product center coatings Covestro. (2018). Bayhydrol® UH 240. Retrieved February 12, 2018, from

https://www.coatings.covestro.com/en/Products/Bayhydrol/ProductListBayhydrol/201503030528/Bayhydrol-UH-240

Sehaqui, H., Ezekiel Mushi, N., Morimune, S., Salajkova, M., Nishino, T., & Berglund, L. A. (2012). Cellulose nanofiber orientation in nanopaper and nanocomposites by cold drawing. *ACS Applied Materials and Interfaces*, *4*(2), 1043–1049. http://doi.org/10.1021/am2016766

Sehaqui, H., Zimmermann, T., & Tingaut, P. (2014). Hydrophobic cellulose nanopaper through a mild esterification procedure. *Cellulose*, *21*(1), 367–382. http://doi.org/10.1007/s10570-013-0110-5

Sethi, J., Farooq, M., Sain, S., Sain, M., Sirviö, J. A., Illikainen, M., & Oksman, K. (2018). Water resistant nanopapers prepared by lactic acid modified cellulose nanofibers. *Cellulose*, *25*(1), 259–268. http://doi.org/10.1007/s10570-017-1540-2

Sethi, J., Oksman, K., Illikainen, M., & Sirviö, J. A. (2018). Sonication-assisted surface modification method to expedite the water removal from cellulose nanofibers for use in nanopapers and paper making. *Carbohydrate Polymers*, *197*(October), 92–99. http://doi.org/10.1016/j.carbpol.2018.05.072

Subramani, S., Cheong, I. W., & Kim, J. H. (2004). Chain extension studies of water-borne polyurethanes from methyl ethyl ketoxime/??-caprolactam-blocked aromatic isocyanates. *Progress in Organic Coatings*, *51*(4), 329–338. http://doi.org/10.1016/j.porgcoat.2004.08.004

Tennebroek, R., van der Hoeven-van Casteren, I., Swaans, R., van der Slot, S., Stals, P. J. M., Tuijtelaars, B., & Koning, C. (2018). Water-based polyurethane dispersions. *Polymer International*.

Yang, X. F., Vang, C., Tallman, D. E., Bierwagen, G. P., Croll, S. G., & Rohlik, S.

(2001). Weathering degradation of a polyurethane coating. *Polymer Degradation and Stability*, *74*(2), 341–351. http://doi.org/10.1016/S0141-3910(01)00166-5

Yoon Jang, J., Kuk Jhon, Y., Woo Cheong, I., & Hyun Kim, J. (2002). Effect of process variables on molecular weight and mechanical properties of water-based polyurethane dispersion. *Colloids and Surfaces A: Physicochemical and Engineering Aspects*, *196*(2–3), 135–143. http://doi.org/10.1016/S0927-7757(01)00857-3